

Structural Remodeling Analysis of Induced Arrhythmias in Rabbit Heart

Mouhamed Zakiou Kolawole Adissa Raimi^{1,2}, Saleem Ullah¹, Pamela Pinheiro Martins¹, Antoine Joao Jacques Gerber¹, Fernanda Fogaça Ruiz¹, Marcela Sorelli Carneiro Ramos¹, Silvia Honda Takada¹, João Salinet¹

Federal University of ABC, Brazil¹ University of Abomey Calavi, Benin²

Abstract

Cardiac arrhythmias, including fibrillation and tachycardia, are characterized by interrupted electrical conduction and increased interstitial fibrosis. This study examines histological changes in rabbit hearts with induced arrhythmias. Four New Zealand White rabbits (3-4 kg) were divided into control (n = 1) and experimental (n = 3) groups. Isolated hearts underwent Langendorff perfusion and arrhythmias were produced using 1 μ M carbachol and an S1-S2 procedure (100 bursts, 2 ms pulses, 1.3 s intervals). Following electrophysiological evaluation, hearts were formalin-fixed, and samples were taken from three distinct atrial and ventricular regions. Three slices per region (2-3 sections, 5 μ m thick) were stained with hematoxylin and eosin to assess tissue integrity and remodeling. Quantitative image analysis revealed structural variations across groups.

The control group showed preserved cardiac architecture, whereas arrhythmic hearts exhibited increased interstitial fibrosis and cardiomyocyte hypertrophy, most evident in ventricular fibrillation. This study highlights distinct structural alterations associated with atrial and ventricular arrhythmias. Ongoing analyses will correlate these histological changes with simultaneous panoramic optical and epicardial electrical mapping.

1. Introduction

Cardiac arrhythmias, including atrial tachycardia (AT) and ventricular fibrillation (VF), are major contributors to cardiovascular morbidity and mortality. Beyond electrical disturbances, they involve profound structural remodeling, notably interstitial fibrosis and cardiomyocyte hypertrophy, which foster arrhythmogenic substrates sustaining abnormal conduction circuits [1]. Fragmented conduction, reentry phenomena, and heterocellular coupling further reinforce this pathological remodeling [2]. Fibrosis disrupts myocardial conductivity by increasing intercellular resistance and promoting

anisotropic conduction [3,9]. Concurrently, ultrastructural changes—including mitochondrial damage, cytoskeletal disorganization, and impaired gap junctions—undermine contractility and synchrony [4,10]. Despite extensive research, the bidirectional relationship between electrical dysfunction and remodeling remains incompletely understood, particularly in acute experimental settings.

In this study, we employed a rabbit model to investigate the histological changes associated with arrhythmia induction using carbachol and programmed electrical stimulation. Using classical histology, we aimed to identify the cellular and subcellular correlates of different arrhythmogenic remodeling and quantify differences between control and arrhythmic hearts. These findings provide a general presentation of architectural renovation of the induced arrhythmias and contribute to ongoing efforts to correlate structural remodeling with electrical and optical mapping data and arrhythmia dynamics.

2. Materials and Methods

2.1. Animal Preparation and Heart Perfusion

The study was approved by the Ethics Committee on the Use of Animals of the Federal University of ABC in São Paulo, Brazil, under protocol 3947230519.

Four adult New Zealand White rabbits (3–4 kg) were divided into two groups: control (n = 1) and experimental (n = 3). Hearts were excised under deep anesthesia and mounted on a Langendorff perfusion apparatus using oxygenated Krebs-Henseleit buffer, as previously described [5].

2.2. Arrhythmia Induction Protocol

Arrhythmias were pharmacologically and electrically induced in the experimental groups. Each heart was perfused with 1 μ M carbachol, a muscarinic agonist that increases parasympathetic tone and lowers atrial refractory periods. This was followed by S1-S2

programmed stimulation (100 bursts of 2 ms pulses at 1.3 s intervals) to induce arrhythmias such as atrial and ventricular tachycardia and escalate to fibrillation [5,6]. The control heart underwent identical handling and perfusion without carbachol or electrical stimulation.

2.3. Histological Analysis

After consistent anatomical orientation, care was taken to the perfused hearts orientation in the Langendorff system, photos and videos were taken including the MEAs positions.

Subsequently, the electrophysiological protocol, heart orientation was kept, and three tissue samples per perfused heart were made at the MEAs areas (MEA 1: Left atrium, MEA 2: ventricle and MAE 3: right atrium (Fig.1 a), marked on the tissue with sharp needle or blade. Tissue samples of the control heart were collected from four anatomical regions: right atrium, left atrium, right ventricle, and left ventricle. Afterward samples were put in histological cassettes with the same orientation and kept fixed in 10% formalin for 48 hours. The tissue piece was mounted in the metal mold putting epicardium-side down to ensure maximum longitudinal alignment of muscle fibers with the slicing plane. Three slices from each sample were prepared, and 5 μ m tangential to the epicardium surface sections thick were obtained [7].

Hematoxylin and eosin (H&E) staining was done to assess general tissue integrity and cell morphology [8]. Parameters assessed included nucleus density (number of myocardial nuclei), myocardial hypertrophy, inter cellular space, and mononuclear cells infiltration. Cardiomyocytes disarray is also a factor of hypertrophy or myocyte loss and is often accompanied by fibrosis. Myocytes should be parallel in heath tissue and in nonhealthy it is dispersed and disorganized parallelism or oblique fiber. Images J was used to count the nucleus and hypertrophic myocardial fibers. Other parameters were analyzed and quantified as minimal (0), mild (1), moderate (2) and severe (3) [7,9,10].

2.4. Statistical Analysis

Statistical analysis was descriptive. Boxplots were generated to depict the distribution of values, including medians, interquartile ranges, and extreme values for each group. This graphical representation was chosen to facilitate visual comparison of variability without formal hypothesis testing. All analyses and plots were performed using Statistical Package for the Social Sciences for Windows (SPSS 22.0, IBM SPSS Inc.) and GraphPad Prism 10.

3. Results

Using the prementioned protocol, we were able to induce arrhythmias, such as atrial tachycardia, ventricular tachycardia and ventricular fibrillation in the perfused hearts.

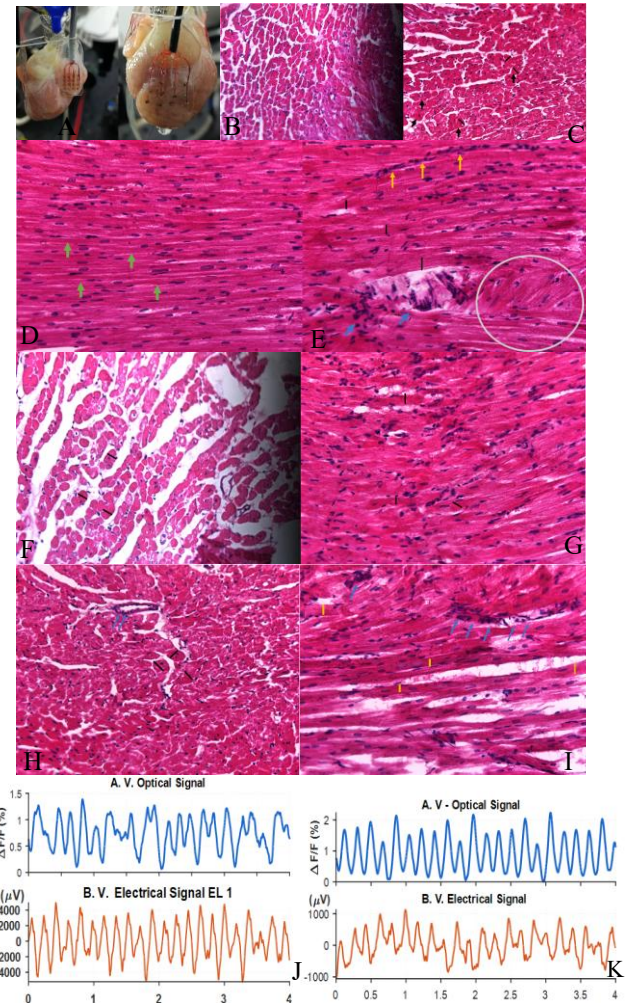


Fig. 1: Atriums and ventricles images (H & E x 20, Scale bar 500 μ m). (A) perfused heart in Langendorff system. (B) atrium control heart and (C) atrium perfused heart under ventricular fibrillation, showing hypertrophic fibers. (D) ventricle control heart and (E) ventricle perfused heart under ventricular fibrillation showing hypertrophic fibers: black arrows, clusters of nuclei: blue arrows, mononuclear cells infiltration: yellow arrows and cardiomyocytes fibers disarrays: gray circle. (F) atrium of perfused heart under atrial tachycardia showing more increased intra cellular space, (G) ventricle of perfused heart under atrial tachycardia showing myocardial hypertrophic fibers and increased nucleus. (H) atrium of perfused heart under atrial tachycardia showing mononuclear cell infiltration: blue arrows and hypertrophic fibers black arrows. (I) ventricle of perfused heart under ventricular fibrillation and ventricular tachycardia. (J) A.V. Optical Signal ($\Delta F/F$ %) and (K) B.V. Electrical Signal (μ V) over time (0 to 4 seconds).

tachycardia depicting mononuclear cells infiltration: blue arrows, myocardial hypertrophic fibers: yellow arrows and increased intra cellular space. (J, K) optical and electrical signal plots of the perfused hearts under fibrillation.

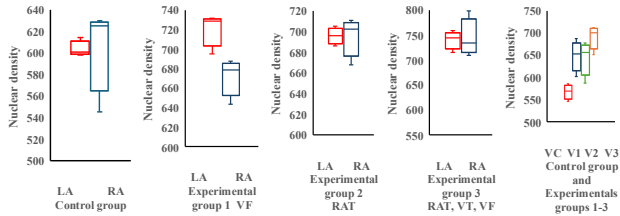


Fig. 2: Boxplots of nucleus density in the atrium and ventricle among control and experimental groups.

Table 1.: Histological markers of the (R/L) atriums in control and experimental groups of (VF: Ventricular Fibrillation, RAT: Right atrium tachycardia, VT: Ventricular tachycardia)

Groups	Atriums control group	Atriums group 1: VF	Atriums group 2: RAT	Atriums group 3: RAT+VT+VF
Histological parameters	R L	R L	R L	R L
Inter cellular space	Minimal(0)	Mild (1)	Moderate (2)/Mild (1)	Mild (1)
Myofibers disarrays	Minimal(0)	Mild (1)	Mild (1)	Mild (1)
Clusters of nuclei	Minimal(0)	Mild (1)	Mild (1)	Mild (1)
Mononuclear cells infiltration	Minimal (0)	Mild (1)	Mild (1)	Mild (1)

Table 2.: Histological parameters of the ventricle in control and experimental groups

Groups	Ventricle control group	Ventricle group1: VF	Ventricle group 2: RAT	Ventricle group3: RAT, VT, VF
Histological parameters	Left Right			
Inter cellular space	Minimal(0)	Mild (1)	Mild (1)	Moderate(2)
Myofibers disarrays	Minimal(0)	Mild (1)	Mild (1)	Moderate(2)
Clusters of nuclei	Minimal(0)	Mild (1)	Mild (1)	Moderate(2)
Mononuclear cells infiltration	Minimal(0)	Mild (1)	Mild (1)	Moderate (2)

4. Discussion

Arrhythmias, particularly those induced by rapid pacing or drugs, create a substrate for both electrical and

structural remodeling [10,11]. Our Rapid pacing models in rabbits, leads to changes in myocardial architecture.

Histological analysis using hematoxylin and eosin staining in rabbit models of induced arrhythmias consistently reveals increased cellularity, expansion of interstitial spaces, and myocyte hypertrophy. These findings are corroborated by studies showing that both atrial and ventricular arrhythmias, when sustained, lead to quantifiable myocardial scarring, fiber disarray, and altered tissue geometry [12,13,14]. The increased density of myocardial nuclei (Fig. 1,2) likely reflects both myocyte hypertrophy and proliferation of non-myocyte cell types, such as fibroblasts and inflammatory cells, which are recruited during the remodeling process [14,15]. The expansion of intracellular space and fiber disarray are indicative of disrupted cell-cell coupling and extracellular matrix remodeling, which are hallmarks of arrhythmogenic substrates [15,16].

The degree of structural remodeling is not uniform across all arrhythmias. Nuclear density and hypertrophy are increased in all perfused hearts compared to non-perfused. Approximatively five percent of the fibers are hypertrophied in all perfused heart. Other parameters including intracellular space, mononuclear cells infiltration and cardiomyocytes fiber disarray are quantified mild (1), expected in fibrillation where it was moderate (2) (Table. 1,2). Fibrillating hearts (Fig.1, j, k), particularly those experiencing ventricular or atrial fibrillation, exhibit the most prominent histopathological changes (Fig.1, e, i). This is consistent with the clinical and experimental observation that Atrial Fibrillation (AF) is both a cause and consequence of atrial remodeling, creating a vicious cycle that perpetuates arrhythmogenicity [11,13,15]. In contrast, other arrhythmias, such as those limited to the atria or ventricles without fibrillation, induce less pronounced but still noticeable remodeling. The greater severity in fibrillating hearts may be attributed to the higher frequency and irregularity of electrical activation, which imposes greater metabolic and mechanical stress on the myocardium, accelerating the remodeling process [13,12,15].

The structural remodeling observed in arrhythmia models has profound functional implications. Myocyte hypertrophy and fiber disarray impair contractile function, while increased fibrosis and altered gap junction expression slow conduction and increase the risk of conduction block and reentry [12,13,15,16]. These changes not only perpetuate arrhythmias but also contribute to the progression of heart failure and adverse clinical outcomes [12,17].

While the rabbit's heart shares many structural and electrophysiological features with the human heart, species differences must be considered when extrapolating findings. Nonetheless, the consistency of remodeling patterns across various models—whether

induced by pacing, drugs, genetic mutations, or pressure overload—underscores the generalizability of these mechanisms [13,12,15]. Although, this is a preliminary study, limitations include induced arrhythmias, propagation of remodeling, particularly the fibrosis, in the tissue studied area.

5. Conclusion

Our findings indicate that arrhythmia induction in rabbit hearts causes substantial structural remodeling, including increased nuclei density, cardiomyocyte hypertrophy, disarray, and immune cell infiltration. These changes were especially prominent in fibrillating hearts, suggesting a relationship between arrhythmias and myocardial remodeling. Such changes provide a morphological basis for future correlations with electrophysiological mapping, as well as prospective treatment targets for preventing or reversing arrhythmogenic structural substrates.

Acknowledgments

We thank TWAS-FAPESP for financial support and UFABC Brazil for the research environment.

References

- [1] Makowiec D, et al. "Heart rhythm insights into structural remodeling in atrial tissue: timed automata approach." *Frontiers in Physiology* 9 (2019): 1859.
- [2] Nguyen MN, et al. "Cardiac fibrosis and arrhythmogenesis." *Comprehensive Physiology* 7.3 (2017): 1009-1049.
- [3] Nguyen, et al. "Cardiac fibrosis and arrhythmogenesis: the road to repair is paved with perils." *Journal of Molecular and Cellular Cardiology* 70 (2014): 83-91.
- [4] Severs NJ, et al. "Remodeling of gap junctions and connexin expression in diseased myocardium." *Cardiovascular Research* 80.1 (2008):9-19.
- [5] Bell RM, et al. "Retrograde heart perfusion: the Langendorff technique of isolated heart perfusion." *Journal of Molecular and Cellular Cardiology* 50.6 (2011): 940-950.
- [6] Siles J, et al. "An integrated platform for 2-D and 3-D optical and electrical mapping of arrhythmias in Langendorff-perfused rabbit hearts." *The Journal of Physiology* (2025).
- [7] Oliván VA, et al. "Minimally invasive system to reliably characterize ventricular electrophysiology from living donors." *Scientific Reports* 10.1 (2020): 19941.
- [8] Raimi MZKA, et al. "Honey and black seed synergistically promote regeneration of oligodendrocytes in cuprizone intoxicated quail brain." *Pakistan Journal of Zoology* 56.3 (2024): 1163.
- [9] Yamaguchi T, et al. "Atrial structural remodeling in patients with atrial fibrillation is a diffuse fibrotic process: evidence from high-density voltage mapping and atrial biopsy." *Journal of the American Heart Association* 11.6 (2022): e024521.
- [10] Takahashi Y, et al. "Histological validation of atrial structural remodelling in patients with atrial fibrillation." *European Heart Journal* 44.35 (2023): 3339-3353.
- [11] Zhong, Si, et al. "Subcutaneous BNP injections in rabbits: A novel approach to mitigate myocardial remodeling in atrial fibrillation." *Discovery Medicine* 36.190 (2024): 2182-2190.
- [12] Chin, Shui Hao, et al. "Autonomic neuro-cardiac profile of electrical, structural and neuronal remodeling in myocardial infarction-induced heart failure." *Journal of Molecular and Cellular Cardiology Plus* 5 (2023):
- [13] Lu, Yen-Yu, et al. "Role of endothelin-1 in right atrial arrhythmogenesis in rabbits with monocrotaline-induced pulmonary arterial hypertension." *International Journal of Molecular Sciences* 23.19 (2022): 10993.
- [14] Roh, Seung-Young, et al. "Molecular signatures of sinus node dysfunction induce structural remodeling in the right atrial tissue." *Molecules and Cells* 43.4 (2020): 408-418.
- [15] Baggett, Brett C., et al. "Myofibroblast senescence promotes arrhythmogenic remodeling in the aged infarcted rabbit heart." *Elife* 12 (2023): e84088.
- [16] Trayanova, Natalia A., et al. "Exploring susceptibility to atrial and ventricular arrhythmias resulting from remodeling of the passive electrical properties in the heart: a simulation approach." *Frontiers in Physiology* 5 (2014): 435.
- [17] Goette, Andreas, and Uwe Lendeckel. "Tachycardia-induced remodeling: atria and ventricles take a different route." *Cardiovascular Research* 63.2 (2004): 194-195.

Address for correspondence:

Mouhamed Zakiou Kolawole Adissa Raimi.

Université fédérale ABC (UFABC)
Alameda da Universidade, s/n - Anchieta
Bloc Zeta, Heart Laboratory 107 and 001A
Code postal 09606-045 - São Bernardo do Campo - SP – BR

Email address: kolaraimi2016@gmail.com